6416–6424 *Nucleic Acids Research, 2006, Vol. 34, No. 22* *Published online 27 November 2006*
doi:10.1093/nar/gkl738

Fabrication and characterization of RNA aptamer microarrays for the study of protein–aptamer interactions with SPR imaging

Yuan Li, Hye Jin Lee and Robert M. Corn*

Department of Chemistry, University of California-Irvine, Irvine, CA 92697, USA

Received June 20, 2006; Revised August 14, 2006; Accepted September 22, 2006

ABSTRACT

RNA microarrays were created on chemically modified gold surfaces using a novel surface ligation methodology and employed in a series of surface plasmon resonance imaging (SPRI) measurements of DNA–RNA hybridization and RNA aptamer–protein binding. Various unmodified single-stranded RNA (ssRNA) oligonucleotides were ligated onto identical 5′-phosphate-terminated ssDNA microarray elements with a T4 RNA ligase surface reaction. A combination of *ex situ* polarization modulation FTIR measurements of the RNA monolayer and *in situ* SPRI measurements of DNA hybridization adsorption onto the surface were used to determine an ssRNA surface density of 4.0×10^{12} molecules/cm^2 and a surface ligation efficiency of 85 ± 10%. The surface ligation methodology was then used to create a five-component RNA microarray of potential aptamers for the protein factor IXa (fIXa). The relative surface coverages of the different aptamers were determined through a novel enzymatic method that employed SPRI measurements of a surface RNase H hydrolysis reaction. SPRI measurements were then used to correctly identify the best aptamer to fIXa, which was previously determined from SELEX measurements. A Langmuir adsorption coefficient of 1.6×10^7 M^{-1} was determined for fIXa adsorption to this aptamer. Single-base variations from this sequence were shown to completely destroy the aptamer–fIXa binding interaction.

INTRODUCTION

The use of RNA aptamers, short synthetic oligonucleotide sequences that bind to proteins, is emerging as a powerful tool for affinity purification, biosensors, drug discovery and medical therapy (1,2). Since the initial efforts in 1990 to develop *in vitro* methods for selecting RNA aptamers from a large combinatorial library (3–5), aptamers have been attracting considerable attention from researchers for their excellent specificity and affinity towards a variety of target molecules including drugs, peptides, proteins and even whole cells (6–9). For example, the US FDA has recently approved for the first time the use of an aptamer in the clinical treatment of neovascular age-related macular degeneration (10).

The coupling of nucleic acid microarray technology with RNA aptamers has obvious benefits for the simultaneous analysis of multiple potential aptamer–protein interactions (11–14). RNA microarrays could be used to screen a pool of potential aptamers for binding affinity to a specific target protein conveniently in a single measurement. Additionally, multiple protein or biomarker targets could be simultaneously identified from a biological sample by a unique adsorption pattern onto an RNA aptamer microarray. Moreover, any proteins bound to an RNA aptamer microarray can be easily removed from the surface by denaturing the aptamer microarray either for re-use of the microarray, or for further protein analysis with additional methods such as mass spectrometry.

Despite the many potential benefits of RNA microarrays, they are not yet widely used. This is most likely due to the difficulty of reproducibly fabricating and maintaining stable and uniform RNA microarrays. Since RNA molecules are more susceptible to enzymatic and chemical degradation as compared with DNA, many of surface attachment chemistries developed for DNA microarrays cannot be directly transferred to RNA microarray fabrication. Currently, most RNA microarray fabrication methods typically employ modified RNA sequences such as biotinylated RNA for immobilization on streptavidin-coated surface (12,13,15), or thiol-modified RNA for covalent attachment onto a maleimide-modified monolayer (16). These modifications can be time-consuming, difficult or costly, and can potentially lead to either cross reaction of RNA aptamers during the fabrication process or the introduction of additional proteins into the microarray. Some researchers have attached unmodified RNA to surfaces by hybridization onto immobilized DNA probes (17,18); RNA microarrays formed by this method cannot endure any rigorous washing or buffer conditions that lead to denaturation of the RNA–DNA heteroduplex.

*To whom correspondence should be addressed. Tel: +1 949 824 1746; Fax: +1 949 824 8571; Email: rcorn@uci.edu

Recently, we have demonstrated that stable RNA microarrays can be created using unmodified single-stranded RNA (ssRNA) by a covalent enzymatic ligation reaction with ssDNA immobilized onto a surface (19). Our initial experiments utilized T4 DNA ligase for the surface ligation reaction; this enzyme unfortunately requires the use of a DNA template that can complicate the fabrication process and limit the surface ligation efficiency. In contrast, the enzyme T4 RNA ligase does not require a template for DNA–RNA ligation in solution (20,21). Can we use this enzyme instead of T4 DNA ligase to simplify the RNA microarray fabrication process? In this paper, we demonstrate the successful fabrication of RNA aptamer microarrays using T4 RNA ligase to catalyze surface RNA–DNA ligation reactions. Although T4 RNA ligase has been widely applied in solution reactions, it is the first time that this enzyme has been used to ligate RNA to DNA in a surface format.

The formation of a stable RNA microarray with the surface ligation chemistry is verified with surface plasmon resonance imaging (SPRI) measurements. SPRI is a multiplexed, surface-sensitive optical technique that uses changes in the local refractive index to detect adsorption onto microarrays (22). SPRI measurements of microarrays have been used extensively for the study of DNA–protein, peptide–protein, protein–carbohydrate and protein–antibody interactions (23–28). We have employed SPRI previously to quantitatively monitor the adsorption of DNA and RNA onto DNA microarrays (29,30). Additional *ex situ* polarization modulation FTIR (PM-FTIR) experiments are used to further confirm the formation of an RNA monolayer.

In addition to the fabrication of ssRNA microarrays with T4 RNA ligase, we have developed a second surface enzyme reaction for the determination of the relative surface densities of the RNA microarray elements. This second characterization reaction utilizes the enzyme RNase H to completely remove the ligated RNA from all of the microarray elements via the hydrolysis of RNA–DNA heteroduplexes on the surface. We have used RNase H previously for the ultrasensitive detection of DNA with SPRI measurements of RNA microarrays (31). In this work, we use SPRI in conjunction with RNase H to measure relative surface densities by the amount of SPRI signal loss at each aptamer array element.

Finally, we demonstrate that SPRI measurements of RNA aptamer microarrays can be used to study aptamer–protein interactions. SPRI has not yet been applied to the multiplexed detection of protein adsorption onto RNA aptamer microarrays, although single channel angle shift SPR measurements have been used to study protein–aptamer binding (15,17,18,32,33). In this paper we employ our RNA–DNA surface ligation chemistry to create a five-component RNA microarray of potential aptamers for protein factor IXa (fIXa) (34). SPRI measurements are then used to select the best aptamer for fIXa out of the five RNA aptamer components.

MATERIALS AND METHODS

Reagents

11-Amino-1-undecanethiol hydrochloride (MUAM; Dojindo), sulfosuccinimidyl 4-(*N*-maleimidomethyl)cyclohexane-1-carboxylate (SSMCC; Pierce), 9-fluorenylmethoxycarbonyl-*N*-hydroxysuccinimide (Fmoc-NHS; Novabiochem) and *N*-hydroxysuccinimidyl ester of methoxypoly (ethylene glycol) propionic acid (MW 2000) (PEG-NHS; Nektar Therapeutics) were all used as received. All unmodified RNA sequences (PAGE purified) were purchased from Dharmacon Research Inc. The DNA anchor probe with 3′-thiol modification and 5′-phosphorylation was obtained commercially from Integrated DNA Technologies and was deprotected and purified using reverse-phase binary elution HPLC. All RNA and DNA sequences are listed in Table 1. Human fIXa (Haematologic Technologies Inc.), RNase H (50 U/μl; Takara Mirus Bio) and T4 RNA ligase (50 U/μl; Epicentre Biotechnology) were all diluted to the desired concentration before use. All laboratory prepared aqueous solutions were autoclaved prior to use.

Table 1. Summary of all DNA and RNA sequences used in RNA microarray fabrication and surface protein–aptamer interaction studies

DNA anchor probe
3′-S-S-$(CH_2)_6$-AAAAAAAAAAAAAAAAAATT-5′-phosphate
Reference RNA (R_{ref})
5′-AGACUCUGACUCAGUG
RNA aptamer (R_T)
5′-UUUGGAAGAUAGCUGGAGAACUAACCAAA$(A)_8$
Human fIXa aptamer
R_A = 5′-AUGGGGACU**AUA**CCGCGUAAUGCUGCCUCCCCAU$(A)_8$
Human fIXa aptamer variants
R_B = 5′-AUGGGGACU**CUA**CCGCGUAAUGCUGCCUCCCCAU$(A)_8$
R_C = 5′-AUGGGGACU**C̄UC̄**CCGCGUAAUGCUGCCUCCCCAU$(A)_8$
R_D = 5′-AUGGGGACU**G̅UG̅**CCGCGUAAUGCUGCCUCCCCAU$(A)_8$
R_E = 5′-GGGAUGGGU**A̅A̅U̅A̅**ACUGUAUGGUGAACCCACCC-AAACUCCCAUGGCUA$(A)_8$

The aptamers R_A and R_E have a conserved AUA sequence in bold; in the aptamers R_B, R_C and R_D, this sequence is modified with the underlined bases. Eight adenosine bases were added to the 3′ end of each RNA aptamer sequence to facilitate the surface ligation reaction.

DNA microrray fabrication

A seven-step chemical modification process described previously was employed to create DNA microarrays (35). A Denton DV-502A metal evaporator was used to deposit thin gold films (45 nm) onto SF-10 glass (Schott Glass) with a 1 nm underlayer of chromium. The gold surfaces were first reacted with the amine-terminated alkanethiol MUAM to form a self-assembled monolayer. This MUAM surface was then reacted with Fmoc-NHS to create a hydrophobic background. Next the Fmoc surface was exposed to UV light with a quartz mask containing 500 μm square features to create bare gold patches within the hydrophobic Fmoc background. The bare gold spots were then reacted with MUAM for 2 h before manually spotting SSMCC onto the MUAM array elements to form a thiol-reactive maleimide-terminated surface. The DNA anchor probe with 3′-thiol modification was then spotted onto the individual SSMCC array elements and allowed to react overnight. Upon completion of the DNA attachment reaction, the 5′-phosphate terminated DNA array was thoroughly rinsed with Millipore water, dried in a nitrogen stream and used immediately for the creation of RNA microarrays.

Creation of RNA microarrays using a surface ssRNA ligation reaction

The 5′-phosphate-terminated DNA microarray was used as the base for ssRNA ligation. Ligation reactions were

performed in pH 7.5 Tris buffer (40 mM Tris–HCl, 10 mM $MnCl_2$, 100 μM ATP and 10 mM DTT). Approximately 30 nl of T4 RNA ligase reaction buffer containing both 0.5 U/μl T4 RNA ligase and 10 μM ssRNA was manually spotted using a pico-pump to each 500 μm × 500 μm DNA array element and allowed to react for 3 h at room temperature. Next the Fmoc was removed with a mildly basic solution to regenerate the amine-terminated surface. This surface was then reacted with PEG-NHS to create a background resistant to non-specific adsorption of biomolecules. The RNA microarray was finally rinsed with Millipore water, dried in a nitrogen stream and used for SPRI measurements.

Surface reaction conditions

For surface DNA hybridization experiments, the RNA microarray was exposed to 500 nM complement DNA diluted in 1 ml of Tris buffer (40 mM Tris–HCl and 10 mM $MgCl_2$, pH 7.5) for 15 min. For RNase H hydrolysis reactions, 1 ml of RNase H buffer (50 mM Tris–HCl, 300 mM KCl, 10 mM $MgCl_2$ and 10 mM DTT, pH 7.8) containing 100 U of RNase H was used to react with the RNA microarray for 20 min. For protein–aptamer affinity interactions, human fIXa was diluted to the desired concentration in HEPES buffer (20 mM HEPES, 150 mM NaCl and 2 mM $CaCl_2$, pH 7.4) and reacted with the RNA aptamer microarrays for at least 10 min. All experiments were performed at room temperature.

PM-FTIR measurements

Commercial gold slides (Evaporated Metal Films; 100 nm of Au with a 5 nm underlayer of Cr) were used for all reactions in PM-FTIR reflection–adsorption spectroscopy (PM-FTIRRAS) experiments. PM-FTIRRAS measurements were performed using a Mattson RS-1 spectrometer and an optical layout described elsewhere (36,37). Spectra were collected using a narrow-band HgCdTe detector by averaging 2000 scans acquired at a resolution of 4 cm^{-1}.

SPR imaging measurements

An SPR imager (GWC Technologies) using near-infrared excitation from an incoherent white light source was used for all *in situ* measurements (29). In brief, p-polarized light is generated by passing the white light beam through a polarizer, and then used to illuminate the prism/thin gold film assembly at a fixed incident angle slightly smaller than the SPR angle. The reflected light then passes through a narrow band-pass filter centered at 830 nm and is collected with a CCD camera. SPRI data were collected using V++ 4.0 (Digital Optics, NZ) and further analyzed using the software NIH Image V.1.63.

RESULTS

Three novel results are presented in this paper: (i) the use of a surface T4 RNA ligation reaction to create RNA microarrays on chemically modified gold surfaces, (ii) the characterization of the relative surface densities of multiple RNA aptamer array elements with an RNase H surface enzymatic reaction and (iii) the application of these RNA microarrays in conjunction with SPR imaging measurements for the simultaneous measurement of multiple aptamer–protein binding events in a microarray format.

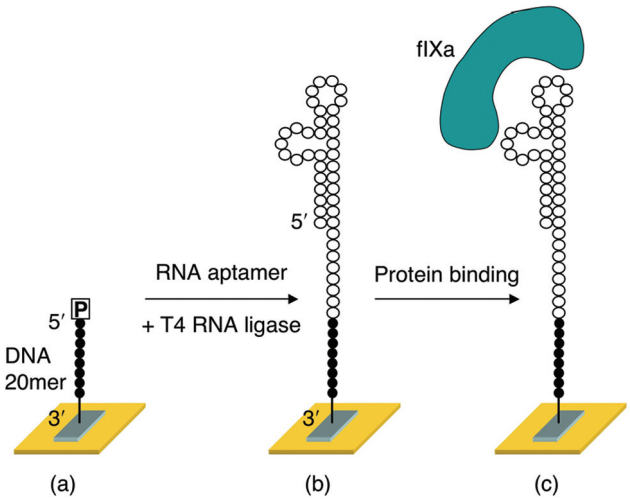

Figure 1. Simplified schematic for the fabrication of RNA aptamer microarrays via RNA–DNA surface ligation chemistry using T4 RNA ligase. DNA bases and RNA bases are shown as closed circles and open circles, respectively. (**a**) The starting microarray consists of 5′-phosphate-terminated ssDNA molecules immobilized on a chemically modified gold surface via a 3′-thiol/surface maleimide reaction. (**b**) Upon exposure to RNA aptamer and T4 RNA ligase, the 3′-hydroxyl of RNA is ligated to the 5′-phosphate of DNA by T4 RNA ligase. Note that eight adenosine bases were added to the 3′ end of the RNA aptamer to facilitate ligation by eliminating the shielding effect caused by hairpin formation. After ligation, the surface is rinsed with 8 M urea to remove the enzyme and non-ligated RNA. (**c**) The RNA microarray can then be used for the study of aptamer–protein affinity interactions.

(i) T4 RNA ligase surface ligation chemistry for RNA microarray fabrication

RNA microarrays were fabricated by attaching unmodified, ssRNA molecules onto ssDNA array elements with a surface T4 RNA ligase reaction as shown schematically in Figure 1. First, a DNA microarray was fabricated by attaching a 3′-thiol modified, 5′-phosphorylated ssDNA 20mer [5′-PO_4^{2-}-T_2A_{18}-$(CH_2)_6$-HS] to each array element via a surface thiol/maleimide reaction that has been described previously (Figure 1a) (35). Each RNA sequence was then directly spotted onto an ssDNA array element using ∼30 nl of a 10 μM target ssRNA solution that also contained ∼0.015 U of T4 RNA ligase (see Materials and Methods for reaction details). The array was allowed to react for 3 h and subsequently rinsed with water and 8 M urea to remove any enzyme and non-ligated ssRNA from the surface. The resulting ssRNA array elements (Figure 1b) were ready for protein–aptamer binding measurements (Figure 1c).

The efficiency of the surface ligation reaction and the bioactivity of the RNA microarrays formed with this fabrication methodology were determined with two different spectroscopic experiments: (i) *ex situ* PM-FTIR measurements and (ii) *in situ* SPRI measurements of DNA hybridization adsorption. The PM-FTIR measurements (spectra not shown) used the intensity of the phosphate band from the nucleic acid backbone at 1074 cm^{-1} as a measure of surface density. We have measured the intensity of this band from

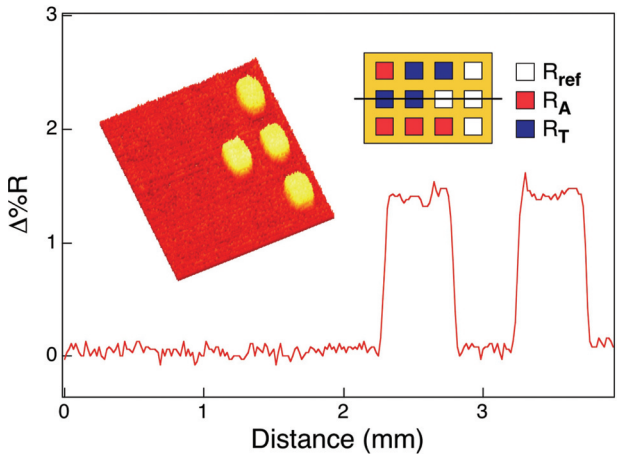

Figure 2. SPRI measurements of DNA hybridization adsorption onto a three-component RNA microarray created by the T4 RNA ligase surface ligation chemistry. The inset on the right shows the pattern of the array. The left inset is an SPRI difference image obtained by subtracting images taken before and after exposure of the array to a 500 nM solution of the DNA complementary to R_{ref}. The line profile taken from the array shows a 1.5% SPRI reflectivity increase at only the R_{ref} array elements due to hybridization adsorption of the complementary DNA. No non-specific adsorption was observed at R_A or R_T array elements, or the PEG background.

ssDNA array elements previously (38); an absorbance of 3.1×10^{-4} corresponding to a DNA surface density of 5.0×10^{12} molecules/cm^2 (30) was observed for a monolayer of the 20mer ssDNA sequence used in the ligation chemistry experiments. A second PM-FTIR spectrum taken after the attachment chemistry exhibited an additional increase in the phosphate band intensity of 2.5×10^{-4} absorbance units. Using these two band intensities, we estimate a ligation efficiency of 80% and an ssRNA surface density of 4.0×10^{12} molecules/cm^2.

To further verify the efficiency of the RNA ligation chemistry, we examined the hybridization adsorption of a complementary DNA sequence onto the RNA microarray. A three-component RNA microarray was created using the T4 RNA surface ligation reaction. Three different ssRNA sequences were attached to the surface: R_A, R_T and R_{ref} in a pattern shown in the inset of Figure 2. The sequences R_A and R_T are known aptamer structures that can form hairpin loops to bind protein molecules, and R_{ref} is a 16mer that does not form any hairpin structures (see Table 1 for the ssRNA sequences). Figure 2 shows the SPRI difference image obtained upon exposure of the RNA microarray to a 500 nM solution of the ssDNA 16mer complement of R_{ref}. A quantitative line profile taken through the center four array elements is also shown in Figure 2. A 1.5 ± 0.1% increase in reflectivity ($\Delta\%R$) was observed for the R_{ref} elements due to the hybridization adsorption of the complementary DNA. Our previous SPRI measurements of hybridization onto ssDNA and ssRNA microarrays formed by 3′-thiol/maleimide attachment chemistry typically show a $\Delta\%R$ of ~1.8% (19). Assuming similar surface hybridization efficiencies, the RNA–DNA ligation efficiency of the surface T4 RNA ligase reaction can be roughly estimated to be 85 ± 10% from these two numbers. This ligation efficiency is the same (within error) as that obtained from the PM-FTIR measurements. Also note that neither DNA adsorption was observed onto the two sets of non-complementary array elements nor the PEG-modified background.

Using the T4 RNA ligase surface chemistry, we next created a five-component ssRNA aptamer microarray. The five ssRNA molecules (labeled R_A–R_E) and the microarray pattern are shown in Figure 3. Each of these ssRNA molecules is based on ssRNA sequences identified previously in a SELEX experiment by Rusconi *et al.* (34). They are loop–stem structures that can potentially bind human fIXa (also see Table 1 for sequences). One of the RNA aptamers, R_A, is the same sequence used in the three-component RNA microarray shown above. As shown in Figure 3, sequence R_A can form two loops, L1 and L2. The sequences R_B, R_C and R_D are modified R_A aptamers with single-base or double-base variations in the L1 loop, and R_E shares a conserved sequence (AUA) in its L1 loop with R_A but differs significantly elsewhere. From the filter-binding measurements, only sequences R_A and R_E are expected to bind to fIXa, with R_A having a stronger binding affinity than R_E (34). Each of the five ssRNA array elements contains an $(A)_8$ sequence at the 3′ end of the molecule. This $(A)_8$ sequence will be used in the next section to determine the relative surface densities of the array elements.

(ii) RNase H surface hydrolysis reaction for measuring relative surface densities

In order to simultaneously determine the relative surface coverages of the different aptamer elements in an RNA microarray, we have developed a unique approach that utilizes SPRI measurements of RNase H surface hydrolysis reactions. We have used RNase H surface reactions previously for the ultrasensitive detection of ssDNA (31). RNase H specifically hydrolyzes the RNA in an RNA/DNA heteroduplex, whereas it does not attack ssRNA, ssDNA, dsRNA or dsDNA. Surface-bound RNA–DNA heteroduplexes such as the one formed by R_{ref} and its DNA complement in the previous section can be hydrolyzed and removed from the surface using RNase H. Indeed, exposure of the three-component array to RNase H after hybridization adsorption resulted in a reflectivity loss in the SPRI difference image for the RNA–DNA heteroduplex array elements due to the removal of the RNA and DNA from the surface (data not shown). We will use this SPRI reflectivity loss experiment to determine the relative surface densities of the various elements in an ssRNA microarray.

A schematic diagram of the relative surface density measurement utilizing RNase H hydrolysis is depicted in Figure 4. Each surface ligated ssRNA molecule contains a single-stranded $(A)_8$ region at its 3′ end (Figure 4a). When the microarray is exposed to a poly-(T) DNA 24mer $(T)_{24}$, the DNA can hybridize to the $(A)_8$ ssRNA sequence and form an RNA/DNA heteroduplex that can be hydrolyzed by RNase H (Figure 4b). The bottom DNA anchor probe has a $(dA)_{18}$ region that also hybridizes to the $(T)_{24}$ (not depicted in the figure), but this DNA/DNA duplex is not attacked by RNase H and the hybridized DNA $(T)_{24}$ can be removed by simply rinsing the array with 8 M urea upon completion of the RNase H reaction. The hydrolysis of the $(A)_8$ stem will cause the entire RNA aptamer to be released from the surface,

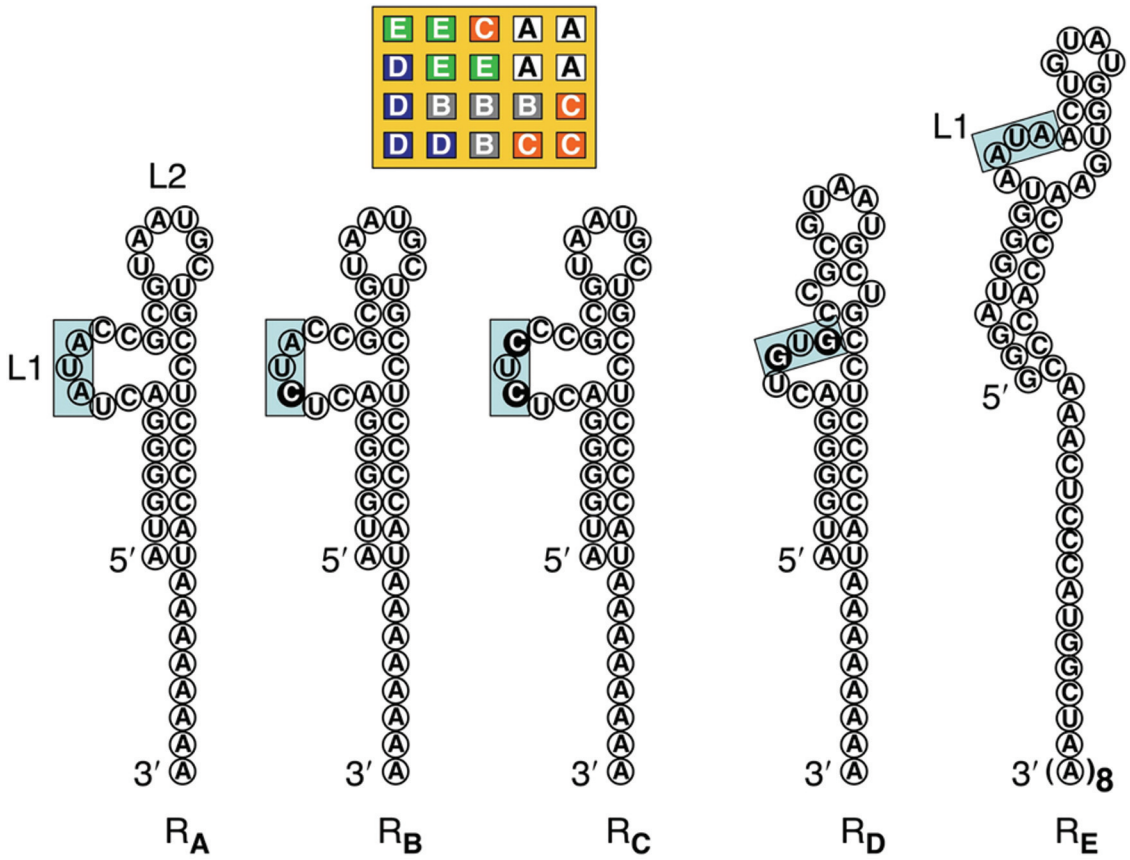

Figure 3. A schematic showing the structures of five different fIXa aptamer variants (R_A–R_E). The pattern shown at the top is the configuration of these five aptamers on an RNA microarray. The AUA sequence in Loop 1 (L1) for R_A and R_E is boxed and the base variations in R_B, R_C, R_D are shown as dark circles. R_B and R_C are variants of R_A with a single-base and double-base variation, respectively, at the AUA sequence that does not change the overall hairpin structure. R_D is a modified R_A aptamer with a double-base variation at the AUA sequence that completely alters the hairpin structure.

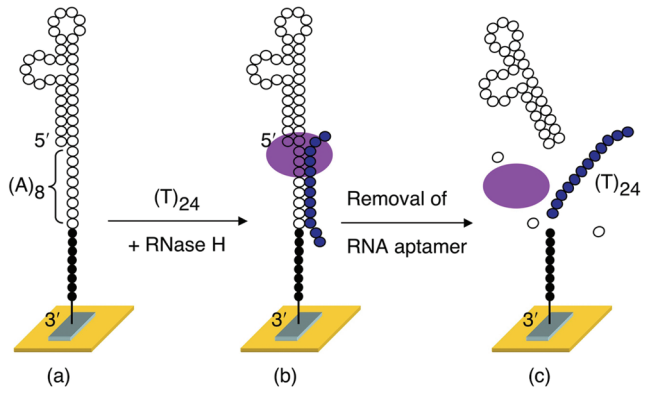

Figure 4. A schematic presentation of the surface RNase H hydrolysis reaction on a surface attached RNA aptamer. DNA bases and RNA bases are shown as closed circles and open circles, respectively. (**a**) The aptamer is attached to the DNA microarray via its 3′-hydroxyl group and has a single-stranded $(A)_8$ spacer arm. In this case, the DNA anchor probe is a 3′-thiol modified, 5′-phosphorylated 20mer [5′-PO_4^{2-}-T_2A_{18}-$(CH_2)_6$-HS]. (**b**) Exposure of the aptamer to a poly-(T) DNA 24mer $(T)_{24}$ results in the formation of a surface heteroduplex that can be hydrolyzed by RNase H. (**c**) RNase H specifically hydrolyzes the $(A)_8$ stem of the RNA aptamer, leading to the complete removal of the RNA aptamer from the surface. The DNA duplex formed between the anchor probe and DNA $(T)_{24}$ is not hydrolyzed by RNase H and can be denatured by 8 M urea upon completion of the RNase H reaction.

while leaving the DNA anchor probe intact (Figure 4c), leading to a loss in SPRI signal. As the intensity of the SPRI signal decrease is directly proportional to the amount of RNA removed from the surface, the measured $\Delta\%R$ quantitatively determine the relative surface coverages of the different RNA aptamers.

This RNase H surface hydrolysis reaction was performed on the five-component RNA microarray described in the previous section to verify that all five of the ssRNA array elements had equal surface densities. The RNA aptamers were hydrolyzed upon exposing the five-component microarray to a solution of RNase H and DNA $(T)_{24}$. The removal of the RNA from the surfaces was detected with SPRI by subtracting images taken before and after the RNase H hydrolysis. Figure 5 shows the results of this RNase H hydrolysis reaction. The array pattern and the SPRI difference image are shown in Figure 5a and b, respectively, and Figure 5c shows the two line profiles taken from the second and fourth rows of the array. In the two line profiles, array elements R_A, R_B, R_C and R_D show similar reflectivity decrease, whereas the loss from sequence R_E is ~25% greater. The additional loss for sequence R_E is due to the fact that sequence R_E is 25% longer (55 bases) than the other RNA sequences R_A–R_E (42 bases). The regular line profiles in Figure 5 verify that each array element contains approximately the same

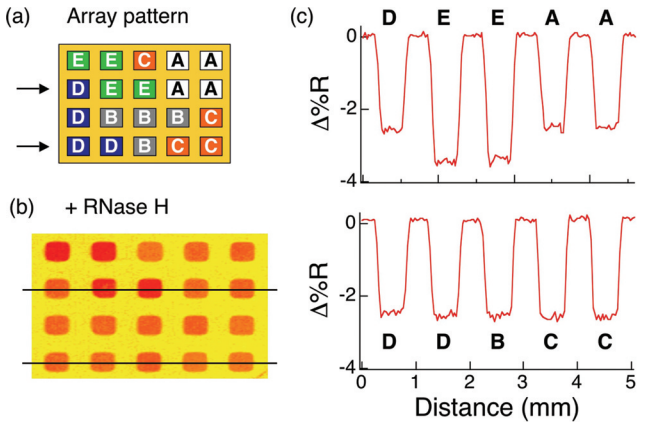

Figure 5. Relative surface density determination by SPRI measurements of the RNase H hydrolysis reaction on a five-component RNA aptamer microarray. (**a**) Pattern of the five RNA aptamers on the array. A–E represents aptamers R_A–R_E respectively. (**b**) An SPRI difference image obtained from the RNase H hydrolysis reaction. An initial SPRI image was taken in the RNase H reaction buffer only. The aptamer microarray was then exposed to a mixture of RNase H and poly-T DNA 24mer $(T)_{24}$ for the complete removal of each aptamer from the surface. Next 8 M urea was used to rinse the array to remove any $(T)_{24}$ that was bound to the DNA anchor probe. Then a second image was taken in the analyte-free RNase H reaction buffer. The initial image was subtracted from the second image to obtain the SPRI difference image. (**c**) The top and bottom line profiles are obtained respectively from the second and fourth rows in the SPRI difference image in (b). SPRI signal losses at array elements D, E and A are displayed in the top line profile and D, B and C are displayed in the bottom line profile. The loss at array element E is 25% greater because the sequence R_E is 25% longer than the sequences R_A–R_D.

number of ssRNA molecules, and confirms the uniformity of the surface density for all of the elements in the microarray.

(iii) SPRI measurements of protein binding to an RNA aptamer microarray

To demonstrate the use of SPRI with RNA aptamer microarrays, the binding of the protein human fIXa to the RNA microarray containing the five potential RNA aptamers in Figure 3 was quantitatively measured. Figure 6 shows the SPRI difference image and a quantitative line profile obtained upon exposure of the microarray to a 100 nM fIXa solution. At this solution concentration, only aptamer array elements R_A and R_E had an observable amount of fIXa adsorption with $\Delta\%R$ of 2.9 and 1.1%, respectively, in the SPRI difference image and line profile (Figure 6). No non-specific adsorption of fIXa was observed on the PEG-modified background. Moreover, no adsorption (either specific or non-specific) of fIXa onto the ssRNA elements R_B, R_C or R_D was observed at any fIXa concentration up to 500 nM. Thus, only two of these ssRNA sequences act as aptamers with a binding affinity for the protein fIXa. The line profile in Figure 6 shows that the R_A aptamer (array element A) has the strongest binding affinity, and aptamer R_E has a weaker but distinct binding affinity for fIXa. These results agree with the previous filter-binding assay measurements (34).

Finally, the adsorption of fIXa to the R_A array elements was quantified using a series of equilibrium SPRI measurements at various fIXa concentrations ranging from 10 to 500 nM. The averaged data points from three separate sets of SPRI measurements are plotted as a function of the

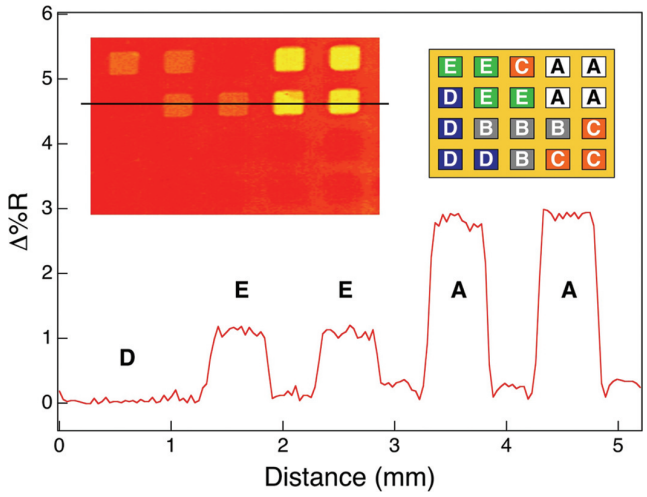

Figure 6. SPRI screening of active fIXa aptamers for fIXa protein binding with a five-component fIXa aptamer array. The array was composed of R_A, R_B, R_C, R_D and R_E with their sequences and structures summarized in Table 1 and Figure 3, respectively. The array pattern is shown in the right inset. The left inset is an SPRI difference image obtained from the adsorption of 100 nM fIXa onto the aptamer array. Significant increase in percent reflectivity was observed only at the R_A and R_E array elements. The line profile obtained from the second row of the difference image demonstrates that the R_A aptamer has a very strong binding affinity, while the R_E aptamer has a weaker affinity to fIXa. The other three fIXa aptamer variants do not have measurable binding affinity to fIXa.

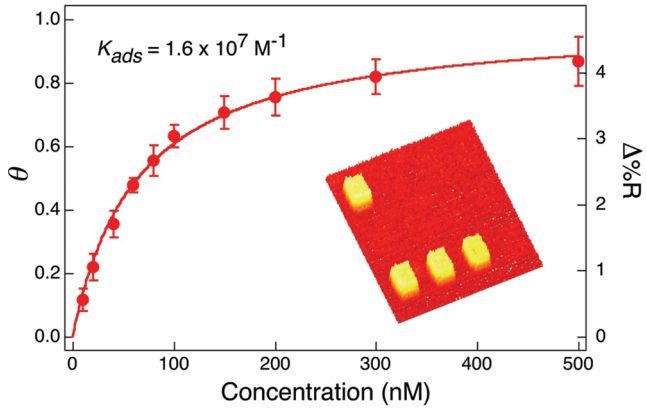

Figure 7. A plot of fractional surface coverage (θ) of fIXa as a function of solution fIXa concentrations ranging from 10 to 500 nM. The surface coverage (θ) was calculated from the value of $\Delta\%R$. Each data point was the average of $\Delta\%R$ measurements from three different arrays. Experimental data are shown as circles and the solid line is the Langmuir isotherm with a surface adsorption constant (K_{ads}) of 1.6×10^7 M^{-1}. The inset is a 3-D SPRI difference image obtained from 20 nM fIXa adsorption onto the R_A array elements of a three-component microarray (see Figure 2 inset for array pattern).

solution fIXa concentration in Figure 7. The inset of Figure 7 is an SPRI difference image obtained from the adsorption of fIXa onto the three-component RNA microarray described in Section (i). The solid line in the figure is a fit of the data points to a Langmuir adsorption isotherm (39):

$$K_{ads}C = \frac{\theta}{1-\theta} \qquad \mathbf{1}$$

where K_{ads} is the Langmuir adsorption coefficient, C is the bulk concentration and θ is the relative surface coverage

which is assumed to be directly proportional to the SPRI reflectivity increase ($\theta = S^*\Delta\%R$, S is an experimentally determined proportionality constant) from Fresnel calculations for $\Delta\%R < 10\%$ (29). A two-component fit (K_{ads} and S) of the data allowed us to determine a Langmuir adsorption coefficient (K_{ads}) of 1.6 ($\pm$0.2) $\times 10^7$ M^{-1}. For comparison with solution affinity constants, this adsorption coefficient can be used to determine the protein concentration at which $\theta = 0.5$ ($C_{0.5\theta} = 1/K_{ads}$); for fIXa-$R_A$ binding, $C_{0.5\theta}$ is equal to 62 nM. It is worth noting that the same K_{ads} was obtained from measurements of RNA microarrays with reduced RNA surface density created by diluting the phosphorylated DNA anchor molecules with non-phosphorylated DNA sequences.

DISCUSSION

(i) T4 RNA ligase surface ligation chemistry for RNA microarray fabrication

The RNA microarray fabrication methodology described here has a number of significant advantages when compared with existing RNA microarray fabrication methods. The first advantage is that the surface ligation strategy uses unmodified ssRNA. This means that both synthetic and *in vitro* transcribed RNA molecules can be readily used for the fabrication process. Conventional RNA microarray fabrication methods often employ biotin or thiol-modified RNA molecules and a chemical surface attachment chemistry similar to that used in the fabrication of DNA microarrays (12,13,16). These chemical modifications to the ssRNA can reduce the stability of the ssRNA, leading to cross reaction of RNA molecules during the fabrication process, and potentially interfere with the RNA aptamer folding and subsequent bioaffinity interactions. Moreover, RNA modification is a non-trivial process that is not only time-consuming and expensive, but cannot be easily incorporated into RNA *in vitro* transcription methods.

The second advantage of this RNA–DNA surface ligation strategy is that it can be used to create high-surface density RNA array elements with a very small amount of ssRNA and standard array spotting technology. The use of a universal ssDNA sequence means that ssDNA can be first attached to all of the array elements in a microarray in one solution reaction, and then the ssRNA probes can be spotted and ligated directly. The T4 RNA ligase reaction has a surface ligation efficiency of 85% or higher, and can create RNA microarray elements with surface densities up to 4×10^{12} molecules/cm^2. The 500 μm array elements used in this paper required 300 fmol of ssRNA per spot for the ligation reaction; fabrication of 50 μm array elements would require only 3 fmol of ssRNA.

A third advantage of this array fabrication strategy is that the RNA microarrays created with the surface ligation chemistry do not contain any background proteins such as streptavidin, making them clean, robust and reusable. Attachment strategies that utilize streptavidin or other proteins have documented problems with non-specific adsorption of target proteins (40,41), and cannot endure harsh washing conditions. The surface ligation reaction allows for facile separation of excess enzyme and reactants by simply rinsing the array. Because the microarray elements only contain covalently linked nucleic acids, target proteins bound to the array can also be easily removed from the surface by rinsing with 8 M urea and then the array can be reused. Moreover, the RNase H hydrolysis reaction can be used to regenerate the phosphorylated ssDNA array and a new RNA microarray can be created on the same substrate (19).

(ii) RNase H surface hydrolysis reaction for measuring relative surface densities

For the accurate measurement of multiple aptamer–protein affinity interactions, it is essential for each array element of the RNA microarray to have comparable and reproducible amounts of aptamers regardless of the different RNA hairpin structures. If this were not the case, signals from target protein binding at different aptamer array elements could not be compared quantitatively. This issue has not been addressed previously with other RNA attachment strategies, but is addressed in this paper with the novel RNase H surface hydrolysis methodology.

The RNase H hydrolysis reaction is a unique and convenient approach for measuring relative surface densities. The key factor in this approach is the $(A)_8$ spacer arm in each RNA aptamer that allows the facile hybridization of $(T)_{24}$ DNA and subsequent hydrolysis by RNase H. The hairpin formation in RNA aptamers makes it difficult to test the amount of RNA present on the surface by directly hybridizing the aptamers with their complementary DNA; however, by using the $(A)_8$ spacer arm and RNase H, the amount of RNA removed from the surface is readily detected by SPRI and therefore provides a good measurement of the relative surface coverages of different RNA aptamers.

For the T4 RNA ligase attachment chemistry, measurements of the relative surface density of different RNA aptamer array elements by RNase H hydrolysis confirmed that the same amount of RNA was ligated to each DNA array element regardless of aptamer hairpin structures. We attribute this consistency in RNA surface density to the long spacer arms placed between the RNA aptamers and the surface that reduce potential steric hindrance. The 20mer DNA anchor probe used in the ligation reaction serves as a spacer in the attachment of RNA aptamers. In addition, eight adenosine bases were added to the 3′ end of each RNA aptamer to elongate the single-stranded region at the 3′-hydroxyl group, which also facilitates the ligation catalyzed by T4 RNA ligase by eliminating the shielding effect caused by hairpin formation. Owing to these two spacer arms, any effect of hairpin structures on the ligation reaction is minimized.

The RNA–DNA surface ligation methodology and RNase H hydrolysis reaction described here were used for gold-modified surfaces and SPRI measurements. However, both are compatible in principle with any ssDNA microarray on a variety of surfaces such as glass, silicon and polymer matrices. We expect that this RNA attachment methodology will find additional application on these substrates in order to take advantage of the various well-characterized DNA microarray attachment and fabrication methodologies that are currently available (42–46).

(iii) SPRI measurements of protein binding to an RNA aptamer microarray

The application of RNA microarrays in conjunction with SPRI for the rapid screening and selection of potential RNA aptamers was demonstrated with the protein fIXa involved in the blood coagulation process. The use of RNA aptamer microarrays allows for the simultaneous SPRI analysis of multiple RNA aptamers on the surface, as compared with single channel angle shift SPR measurements. A single SPRI measurement identified the best aptamer for fIXa from a set of five potential candidates. The SPRI measurement also showed that changing a single base in the RNA sequence could completely destroy the aptamer activity. This suggests that as well as screening aptamers with high affinities, SPRI measurements can be used to identify the active binding site in an RNA aptamer.

In addition to the selection of aptamers, SPRI measurements of RNA microarrays can also be used for the direct detection of multiple proteins from biological samples. A particular protein would be identified by its unique pattern of simultaneous adsorption onto multiple RNA aptamer array elements. The sensitivity of detection of proteins by SPRI with these RNA microarrays is primarily limited by the Langmuir adsorption coefficient for adsorption of the protein to the surface. The creation of RNA aptamers with higher binding affinities will increase the sensitivity of the multiplexed SPRI measurements. Additional sensitivity for the detection of both proteins at very low concentrations and smaller molecules (<10 kDa) can also be achieved by using a sandwich assay format similar to those required for fluorescence measurements. These sandwich assays include the use of nanoparticle-amplified methodologies (47,48) that we recently employed in SPRI measurements for single nucleotide polymorphism identification and detection (49). A future challenge will be the development of microarrays with a sufficiently large number of RNA aptamer array elements to identify and detect multiple related proteins.

ACKNOWLEDGEMENTS

This research was funded by the National Institute of Health (2RO1 GM059622-04) and the National Science Foundation (CHE-0551935). Funding to pay the Open Access publication charges for this article was provided by the NIH.

Conflict of interest statement. None declared.

REFERENCES

1. Bunka,D.H.J. and Stockley,P.G. (2006) Aptamers come of age—at last. *Nat. Rev. Microbiol.*, **4**, 588–596.
2. Proske,D., Blank,M., Buhmann,R. and Resch,A. (2005) Aptamers—basic research, drug development, and clinical applications. *Appl. Microbiol. Biotechnol.*, **69**, 367–374.
3. Ellington,A.D. and Szostak,J.W. (1990) *In vitro* selection of RNA molecules that bind specific ligands. *Nature*, **346**, 818–822.
4. Robertson,D.L. and Joyce,G.F. (1990) Selection *in vitro* of an RNA enzyme that specifically cleaves single-stranded DNA. *Nature*, **344**, 467–468.
5. Tuerk,C. and Gold,L. (1990) Systematic evolution of ligands by exponential enrichment: RNA ligands to bacteriophage T4 DNA polymerase. *Science*, **249**, 505–510.
6. Brody,E.N. and Gold,L. (2000) Aptamers as therapeutic and diagnostic agents. *Rev. Mol. Biotechnol.*, **74**, 5–13.
7. Wallace,S.T. and Schroeder,R. (1998) *In vitro* selection and characterization of streptomycin-binding RNAs: recognition discrimination between antibiotics. *RNA*, **4**, 112–123.
8. Proske,D., Hofliger,M., Soll,R.M., Beck-Sickinger,A.G. and Famulok,M. (2002) A Y2 receptor mimetic aptamer directed against neuropeptide Y. *J. Biol. Chem.*, **277**, 11416–11422.
9. Lupold,S.E., Hicke,B.J., Lin,Y. and Coffey,D.S. (2002) Identification and characterization of nuclease-stabilized RNA molecules that bind human prostate cancer cells via the prostate-specific membrane antigen. *Cancer Res.*, **62**, 4029–4033.
10. Ng,E.W.M., Shima,D.T., Calias,P., Cunningham,E.T., Guyer,D.R. and Adamis,A.P. (2006) Pegaptanib, a targeted anti-VEGF aptamer for ocular vascular disease. *Nat. Rev. Drug Discov.*, **5**, 123–132.
11. Bock,C., Coleman,M., Collins,B., Davis,J., Foulds,G., Gold,L., Greef,C., Heil,J., Heilig,J.S., Hicke,B. *et al.* (2004) Photoaptamer arrays applied to multiplexed proteomic analysis. *Proteomics*, **4**, 609–618.
12. McCauley,T.G., Hamaguchi,N. and Stanton,M. (2003) Aptamer-based biosensor arrays for detection and quantification of biological macromolecules. *Anal. Biochem.*, **319**, 244–250.
13. Cho,E.J., Collett,J.R., Szafranska,A.E. and Ellington,A.D. (2006) Optimization of aptamer microarray technology for multiple protein targets. *Anal. Chim. Acta*, **564**, 82–90.
14. Kirby,R., Cho,E.J., Gehrke,B., Bayer,T., Park,Y.S., Neikirk,D.P., McDevitt,J.T. and Ellington,A.D. (2004) Aptamer-based sensor arrays for the detection and quantitation of proteins. *Anal. Chem.*, **76**, 4066–4075.
15. Murphy,M.B., Fuller,S.T., Richardson,P.M. and Doyle,S.A. (2003) An improved method for the *in vitro* evolution of aptamers and applications in protein detection and purification. *Nucleic Acids Res.*, **31**, e110.
16. Goodrich,T.T., Lee,H.J. and Corn,R.M. (2004) Enzymatically amplified surface plasmon resonance imaging method using RNase H and RNA microarrays for the ultrasensitive detection of nucleic acids. *Anal. Chem.*, **76**, 6173–6178.
17. Misono,T.S. and Kumar,P.K.R. (2005) Selection of RNA aptamers against human influenza virus hemagglutinin using surface plasmon resonance. *Anal. Biochem.*, **342**, 312–317.
18. Mori,T., Oguro,A., Ohtsu,T. and Nakamura,Y. (2004) RNA aptamers selected against the receptor activator of NF-κB acquire general affinity to proteins of the tumor necrosis factor receptor family. *Nucleic Acids Res.*, **32**, 6120–6128.
19. Lee,H.J., Wark,A.W., Li,Y. and Corn,R.M. (2005) Fabricating RNA microarrays with RNA–DNA surface ligation chemistry. *Anal. Chem.*, **77**, 7832–7837.
20. Tessier,D.C., Brousseau,R. and Vernet,T. (1986) Ligation of single-stranded oligodeoxyribonucleotides by T4 RNA ligase. *Anal. Biochem.*, **158**, 171–178.
21. Brennan,C.A., Manthey,A.E. and Gumport,R.I. (1983) Using T4 RNA ligase with DNA substrates. *Methods Enzymol.*, **100**, 38–52.
22. Brockman,J.M., Nelson,B.P. and Corn,R.M. (2000) SPR imaging measurements of ultrathin organic films. *Annu. Rev. Phys. Chem.*, **51**, 41–63.
23. Wolf,L.K., Fullenkamp,D.E. and Georgiadis,R.M. (2005) Quantitative angle-resolved SPR imaging of DNA–DNA and DNA–drug kinetics. *J. Am. Chem. Soc.*, **127**, 17453–17459.
24. Kyo,M., Usui-Aoki,K. and Koga,H. (2005) Label-free detection of proteins in crude cell lysate with antibody arrays by a surface plasmon resonance imaging technique. *Anal. Chem.*, **77**, 7115–7121.
25. Kanda,V., Kariuki,J.K., Harrison,D.J. and McDermott,M.T. (2004) Label-free reading of microarray-based immunoassays with surface plasmon resonance imaging. *Anal. Chem.*, **76**, 7257–7262.
26. Shumaker-Parry,J.S. and Campbell,C.T. (2004) Quantitative methods for spatially resolved adsorption/desorption measurements in real time by surface plasmon resonance microscopy. *Anal. Chem.*, **76**, 907–917.
27. Smith,E.A. and Corn,R.M. (2003) Surface plasmon resonance imaging as a tool to monitor biomolecular interactions in an array based format. *Appl. Spectrosc.*, **57**, 320A–332A.
28. Wegner,G.J., Lee,H.J. and Corn,R.M. (2002) Characterization and optimization of peptide arrays for the study of epitope–antibody

interactions using surface plasmon resonance imaging. *Anal. Chem.*, **74**, 5161–5168.
29. Nelson,B.P., Grimsrud,T.E., Liles,M.R., Goodman,R.M. and Corn,R.M. (2001) Surface plasmon resonance imaging measurements of DNA and RNA hybridization adsorption onto DNA microarrays. *Anal. Chem.*, **73**, 1–7.
30. Lee,H.J., Li,Y., Wark,A.W. and Corn,R.M. (2005) Enzymatically amplified surface plasmon resonance imaging detection of DNA by exonuclease III digestion of DNA microarrays. *Anal. Chem.*, **77**, 5096–5100.
31. Goodrich,T.T., Lee,H.J. and Corn,R.M. (2004) Direct detection of genomic DNA by enzymatically amplified SPR imaging measurements of RNA microarrays. *J. Am. Chem. Soc.*, **126**, 4086–4087.
32. Tombelli,S., Minunni,M., Luzi,E. and Mascini,M. (2005) Aptamer-based biosensors for the detection of HIV-1 Tat protein. *Bioelectrochemistry*, **67**, 135–141.
33. Baldrich,E., Restrepo,A. and O'Sullivan,C.K. (2004) Aptasensor development: elucidation of critical parameters for optimal aptamer performance. *Anal. Chem.*, **76**, 7053–7063.
34. Rusconi,C.P., Scardino,E., Layzer,J., Pitoc,G.A., Ortel,T.L., Monroe,D. and Sullenger,B.A. (2002) RNA aptamers as reversible antagonists of coagulation factor IXa. *Nature*, **419**, 90–94.
35. Brockman,J.M., Frutos,A.G. and Corn,R.M. (1999) A multi-step chemical modification procedure to create DNA arrays on gold surfaces for the study of protein–DNA interactions with surface plasmon resonance imaging. *J. Am. Chem. Soc.*, **121**, 8044–8051.
36. Barner,B.J., Green,M.J., Saez,E.I. and Corn,R.M. (1991) Polarization modulation FTIR reflectance measurements of thin films and monolayers at metal surfaces utilizing real-time sampling electronics. *Anal. Chem.*, **63**, 55–60.
37. Green,M.J., Barner,B.J. and Corn,R.M. (1991) Real-time sampling electronics for double modulation experiments with fourier transform infrared spectrometers. *Rev. Sci. Instrum.*, **62**, 1426–1430.
38. Smith,E.A., Wanat,M.J., Cheng,Y., Barreira,S.V.P., Frutos,A.G. and Corn,R.M. (2001) Formation, spectroscopic characterization and application of sulfhydryl-terminated alkanethiol monolayers for the chemical attachment of DNA onto gold surfaces. *Langmuir*, **17**, 2502–2507.
39. Adamson,A.W. and Gast,A.P. (1997) *Physical Chemistry of Surfaces, 6th edn*. John Wiley & Sons Inc., NY.
40. Perret,E., Leung,A., Morel,A., Feracci,H. and Nassoy,P. (2002) Versatile decoration of glass surfaces to probe individual protein–protein interactions and cellular adhesion. *Langmuir*, **18**, 846–854.
41. Ruiz-Taylor,L.A., Martin,T.L., Zaugg,F.G., Witte,K., Indermuhle,P., Nock,S. and Wagner,P. (2001) Monolayers of derivatized poly(L-lysine)-grafted poly(ethylene glycol) on metal oxides as a class of biomolecular interfaces. *Proc. Natl Acad. Sci. USA*, **98**, 852–857.
42. Albert,T.J., Norton,J., Ott,M., Richmond,T., Nuwaysir,K., Nuwaysir,E.F., Stengele,K.-P. and Green,R.D. (2003) Light-directed 5′–3′ synthesis of complex oligonucleotide microarrays. *Nucleic Acids Res.*, **31**, e35.
43. Zhong,X.B., Leng,L., Beitin,A., Chen,R., McDonald,C., Hsiao,B., Jenison,R.D., Kang,I., Park,S.-H., Lee,A. *et al.* (2005) Simultaneous detection of microsatellite repeats and SNPs in the macrophage migration inhibitory factor (MIF) gene by thin-film biosensor chips and application to rural field studies. *Nucleic Acids Res.*, **33**, e121.
44. Wei,F., Sun,B., Guo,Y. and Zhao,X. (2002) Monitoring DNA hybridization on alkyl modified silicon surface through capacitance measurement. *Biosens. Bioelectron.*, **18**, 1157–1163.
45. Lu,M., Knickerbocker,T., Cai,W., Yang,W., Hamers,R.J. and Smith,L.M. (2004) Invasive cleavage reactions on DNA-modified diamond surfaces. *Biopolymers*, **73**, 606–613.
46. Manning,M. and Redmond,G. (2005) Formation and characterization of DNA microarrays at silicon nitride substrates. *Langmuir*, **2005**, 395–402.
47. He,L., Musick,M.D., Nicewarner,S.R., Salinas,F.G., Benkovic,S.J., Natan,M.J. and Keating,C.D. (2000) Colloidal Au-enhanced surface plasmon resonance for ultrasensitive detection of DNA hybridization. *J. Am. Chem. Soc.*, **122**, 9071–9077.
48. Lyon,L.A., Musick,M.D. and Natan,M.J. (1998) Colloidal Au-enhanced surface plasmon resonance immunosensing. *Anal. Chem.*, **70**, 5177–5183.
49. Li,Y., Wark,A.W., Lee,H.J. and Corn,R.M. (2006) Single-nucleotide polymorphism genotyping by nanoparticle-enhanced surface plasmon resonance imaging measurements of surface ligation reactions. *Anal. Chem.*, **78**, 3158–3164.